

ANTICORROSIVE COATING OF STEEL WITH HYBRID OXIDE/PORPHYRIN SANDWICH LAYERS DEPOSITED BY DROP CASTING METHOD

VAIDA Mirela¹, BIRDEANU Mihaela¹, LASCU Anca², PALADE Anca², FRINGU Ionela²,
FAGADAR - COSMA Eugenia²

¹National Institute for Research and Development in Electrochemistry and Condensed Matter, Timisoara, Romania, EU

²Institute of Chemistry Timisoara of the Romanian Academy, Timisoara, Romania, EU

Abstract

This paper presents some results of the study regarding the corrosion inhibition properties evaluated in HCl environment of drop casting deposited layers on steel, using ZnV₂O₆ oxide (obtained by hydrothermal and co-precipitation methods) and two Zn-metalloporphyrins, namely: Zn-5-pyridyl-10,15,20-tris(3,4-dimethoxyphenyl)-porphyrin (ZnPyDiMeOPP) and Zn-5(3OH-phenyl)-10,15, 20-tris-(3,4-dimethoxyphenyl)-porphyrin (Zn3OHtris34DiMeOPP).

The open circuit potential measurement and potentiodynamic polarization electrochemical technique with Tafel representation were used to investigate the corrosion protection of mixed sandwich deposited layers.

The performed tests revealed that the best corrosion resistance was obtained in the case of the steel coated with hydrothermally obtained ZnV₂O₆ oxide as first layer and Zn-5-pyridyl-10,15,20-tris(3,4-dimethoxyphenyl)-porphyrin (ZnPyDiMeOPP) as the second layer, i. e. 70.58 % inhibition efficiency.

Keywords: Zinc oxides, porphyrin, thin films, AFM, corrosion

1. INTRODUCTION

Steel is an extensively used material in constructions and in many industries, especially in petroleum industry and power plants [1-3]. Although steel presents exceptionally structural and mechanical properties, steel is exposed at intensive corrosion as a result of its interaction with the environment. Due to the fact that corrosion can affect the integrity of the assemblies build from steel, methods to prevent and diminish its corrosion were developed. The coating with corrosion inhibitors is one of these methods (beside electroplating, chromating, anodizing etc.) [1] that is used to decrease the damage produced by this process. The oxide nanomaterial ZnV₂O₆ is already a well-known material considered for potential applications in lithium secondary battery, light emitting diodes [4-5] or rechargeable Na-ion energy storage [6]. Until present ZnV₂O₆ was obtained using various methods of synthesis from melt-quenching method [4], sol-gel method [7] to rheological phase reaction method [5].

Porphyrins are highly recognized as inhibitors that can reduce corrosion rate usually by adsorbing on the surface of the metal to form a compact protective or passive film [8]. Being extended π -electronic systems, porphyrins act as Lewis acids and have been found to possess excellent anticorrosion properties. Besides, porphyrins are chelating agents with strong bonding capability of interaction with metal surfaces [9].

Due to the fact that oxides and porphyrins thin films depositions already proved to possess anticorrosion properties by presenting an excellent degree of inhibition efficiency [10], the aims of this paper is to present results of experimentally investigations regarding inhibition of corrosion of carbon steel in aggressive 0.1 M HCl media by using coatings of ZnV₂O₆ (obtained by hydrothermal or co-precipitation method), and Zn-metalloporphyrins: Zn-5-pyridyl-10,15,20-tris(3,4-dimethoxyphenyl)-porphyrin (ZnPyDiMeOPP) or Zn-5(3OH-phenyl)-10,15, 20-tris-(3,4-dimethoxyphenyl)-porphyrin (Zn3OHtris34DiMeOPP).

2. EXPERIMENTAL PART

2.1. Synthesis

ZnV₂O₆ oxide was synthesized using two synthesis methods: hydrothermal or co-precipitation. The starting precursors were the same for both methods: Zn(CH₃COO)₃·2H₂O (99.99, %) and V₂O₅ (99.99 %) in a 1:1 molar ratio. In the case of the hydrothermal synthesis, to obtain the ZnV₂O₆ oxide a 250°C temperature was used for 12 h, the pH of the solution being established at 12. In case of obtaining ZnV₂O₆ oxide by co-precipitation method the time for the reaction was 1 h at 250°C.

The Zn-metalloporphyrins were obtained by metalation of the corresponding porphyrin bases that were synthesized by multicomponent synthesis procedures, by using two different aldehydes in condensation reaction with pyrrole [11].

2.2. Apparatus

To perform the anticorrosive tests, single and sandwich structures were obtained by drop casting method on carbon steel disks electrode using the obtained ZnV₂O₆ oxides (by different hydrothermal or co-precipitation synthesis methods) and one of the porphyrins.

The passive layers containing nanomaterials (ZnV₂O₆ oxides and / or porphyrins) (see **Table 1**) were deposited through the drop casting method on carbon steel disks (2 mm thick and 10 mm diameter) with the chemical composition: (wt. %) Fe: 98, Si: 0.339, Mn: 0.619, Cu: 0.311, Cr: 0.18, Ni: 0.179, C: 0.165, Al: 0.0309, Mo: 0.0339, Co: 0.0138, W:<0.05, Pb:<0.05, Nb: 0.0023, Ti:<0.005, V:<0.005, Zr:<0.005, P:<0.005 and S:<0.005. Before the depositions the electrode surface was mechanically polished using emery paper, rinsed with double distilled water and degreased with ethanol. For the drop casting method acetone was used. In Table 1 are presented the structure and the combinations of ZnV₂O₆ oxides and of porphyrins which were deposited on carbon steel electrodes (OL). There were listed as ZnV₂O₆ (h) the ZnV₂O₆ oxide obtained by the hydrothermal method and as ZnV₂O₆ (c) the ZnV₂O₆ oxide obtained by the co-precipitation method.

Morphological and topographical analysis of the obtained single and sandwich-like structures were performed by scanning electron microscopy (SEM - Model Inspect S) and atomic force microscopy (AFM - Model Nanosurf® EasyScan 2 Advanced Research) using the noncontact mode cantilever (scan size of 2.3 μm x 2.3 μm).

Table 1 Drop casting thin films depositions

Target material and deposition order	Deposition mode
ZnV ₂ O ₆ (h)	Mono layer
ZnV ₂ O ₆ (c)	Mono layer
ZnPyDiMeOPP	Mono layer
Zn3OHtris34DiMeOPP	Mono layer
ZnV ₂ O ₆ (h) / ZnPyDiMeOPP	Sandwich
ZnV ₂ O ₆ (h) / Zn3OHtris34DiMeOPP	Sandwich
ZnV ₂ O ₆ (c) / ZnPyDiMeOPP	Sandwich
ZnV ₂ O ₆ (c) / Zn3OHtris34DiMeOPP	Sandwich
ZnPy-DiMeOPP / ZnV ₂ O ₆ (h)	Sandwich
ZnPy-DiMeOPP / ZnV ₂ O ₆ (c)	Sandwich
Zn3OHtris34DiMeOPP / ZnV ₂ O ₆ (h)	Sandwich
Zn3OHtris34DiMeOPP / ZnV ₂ O ₆ (c)	Sandwich

The electrochemical measurements used to investigate the anticorrosive properties of samples were performed on a Voltalab Model PGZ 402 potentiostat coupled with a three electrode electrochemical cell consisting of: a platinum wire counter electrode, a saturated calomel electrode as reference electrode and the working electrodes (bare or drop casting modified OL - mounted into a Teflon body to ensure a controlled active surface of 0.28 cm²). The potentiodynamic polarization measurements were performed at 23 °C by sweeping the potential from -1.3 V to -0.6 V, at a scan rate of 1 mV / s. The solution used for the corrosion studies was 0.1 M HCl. The open circuit potential (OCP) of the modified electrodes was monitored for 30 minutes before polarization. The degree of inhibition efficiency *IE* (%) was calculated using the background equations [12].

3. RESULTS AND DISCUSSION

The morphology of the obtained ZnV₂O₆ oxide through the two synthesis methods and of the porphyrins depositions on carbon steel electrodes was investigated using SEM. The SEM micrographs presented in **Figure 1** reveal the formation of spherical agglomerates combined with an irregular morphology of rode shape in the case of ZnV₂O₆ (h) (**Figure 1a**). It also can be observed that the deposited sandwich structures **Figure 1e, f, i and k** preserve the morphology of their corresponding monolayer thin films **Figure 1a**. In the case of ZnV₂O₆ (c), **Figure 1b**, the SEM micrograph reveals a morphology consisting in the formation of an irregular agglomeration, a shape that is preserved in the deposited sandwich structures which contain ZnV₂O₆ (c): **Figure 1g, h, j and l**.

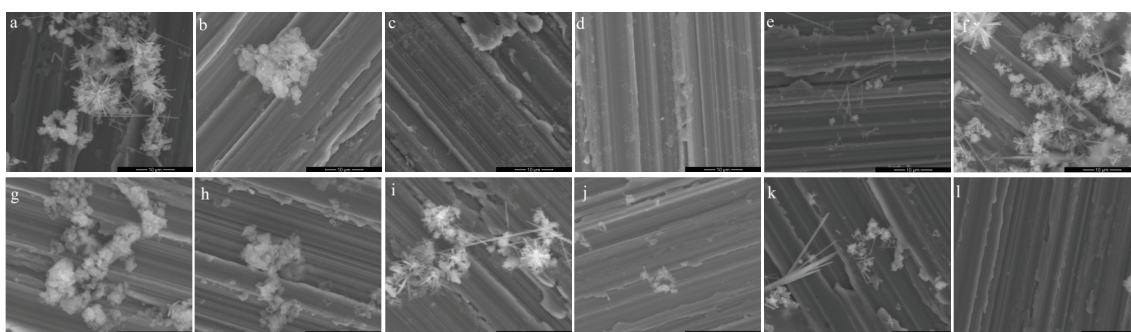


Figure 1 The SEM micrographs of: a) ZnV₂O₆ (h); b) ZnV₂O₆ (c); c) ZnPyDiMeOPP; d) Zn3OHtris34DiMeOPP; e) ZnV₂O₆ (h) / ZnPyDiMeOPP; f) ZnV₂O₆ (h) / Zn3OHtris34DiMeOPP; g) ZnV₂O₆ (c) / ZnPyDiMeOPP; h) ZnV₂O₆ (c) / Zn3OHtris34DiMeOPP; i) ZnPyDiMeOPP / ZnV₂O₆ (h); j) ZnPyDiMeOPP / ZnV₂O₆ (c); k) Zn3OHtris34DiMeOPP / ZnV₂O₆(h); l) Zn3OHtris34DiMeOPP / ZnV₂O₆ (c)

In **Figure 2** are presented the 2D topography for the thin film depositions of ZnV₂O₆ (h), ZnV₂O₆ (c) and of the ZnPy-DiMeOPP and Zn3OHtris34DiMeOPP porphyrins. As in the case of the SEM images, it can be observed that the deposited sandwich structures preserve the morphology of their corresponding mono-layer: **Figure 2e, f, i and k** vs. **Figure 2a** and **Figure 2g, h, j and l** vs. **Figure 2b**. In **Figure 2**, images **c, e, f and g**, where the porphyrin layers are above the oxide it can be seen the specific kwatarion structure of porphyrins aggregates.

From AFM analysis data, using the NanoSurf EasyScan 2 software, were determined the dimensions of the particles that were present on the surface as it can be seen in **Table 2**. The smallest particle dimension, 33 nm, corresponds to the Zn3OHtris34DiMeOPP / ZnV₂O₆ (c) sandwich structure, while the larger dimension of 115 nm appears in the case of the particles presented on the surface of the ZnPyDiMeOPP porphyrin mono layer, that is probably due to the distortion of porphyrin from planar shape to ruffed or saddle conformation. It also were calculated the surface roughness *S_a* - the average roughness, *S_q* - mean square root roughness and *S_y* which represents the layer thickness.

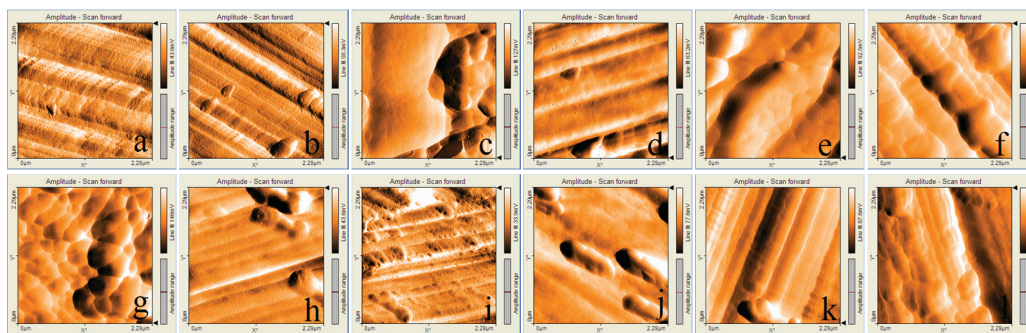


Figure 2 2D AFM surface images of: a) ZnV₂O₆ (h); b) ZnV₂O₆ (c); c) ZnPyDiMeOPP; d) Zn3OHtris34DiMeOPP; e) ZnV₂O₆ (h) / ZnPyDiMeOPP; f) ZnV₂O₆ (h) / Zn3OHtris34DiMeOPP; g) ZnV₂O₆ (c) / ZnPyDiMeOPP; h) ZnV₂O₆ (c) / Zn3OHtris34DiMeOPP; i) ZnPyDiMeOPP / ZnV₂O₆ (h); j) ZnPyDiMeOPP / ZnV₂O₆ (c); k) Zn3OHtris34DiMeOPP / ZnV₂O₆(h); l) Zn3OHtris34DiMeOPP / ZnV₂O₆ (c)

Table 2 Surface particle dimensions and the nano-roughness

Deposited Specimen Type	Particle dimension (nm)	S _a (nm)	S _q (nm)	S _y (μm)
ZnV ₂ O ₆ (h)	71	11	14	0.088
ZnV ₂ O ₆ (c)	29-30	13	16	0.11
ZnPyDiMeOPP	115	37	46	0.26
Zn3OHtris34DiMeOPP	65	12	15	0.11
ZnV ₂ O ₆ (h) / ZnPyDiMeOPP	53	29	37	0.19
ZnV ₂ O ₆ (h) / Zn3OHtris34DiMeOPP	43	18	21	0.13
ZnV ₂ O ₆ (c) / ZnPyDiMeOPP	68	17	21	0.14
ZnV ₂ O ₆ (c) / Zn3OHtris34DiMeOPP	46	11	14	0.098
ZnPyDiMeOPP / ZnV ₂ O ₆ (h)	45	6.7	9.2	0.072
ZnPyDiMeOPP / ZnV ₂ O ₆ (c)	68	13	18	0.13
Zn3OHtris34DiMeOPP / ZnV ₂ O ₆ (h)	65	21	24	0.13
Zn3OHtris34DiMeOPP / ZnV ₂ O ₆ (c)	33	23	29	0.15

In **Figure 3a** are represented the plots for the OCP with time for the investigated electrodes in 0.1 M HCl solution for 30 minutes. As it can be observed, for the sandwich layers structures, the values for potential are higher than for the single layers structures. The curves stabilize after 200 s. The evolution in time of the open circuit potential indicates a shift in free potential toward more negative values.

The Tafel curves (potential vs. log current density) of the modified OL disks with drop casting deposited layers (mono or sandwich structures) recorded in 0.1 M HCl are presented in **Figure 3b**. The Tafel parameters calculated for the investigated electrodes are illustrated in **Table 3**. The highest value for the inhibition efficiency (*IE*), 70.58 %, was obtained in the case of the deposited sandwich structure ZnV₂O₆ (h) / ZnPyDiMeOPP. The corrosion potential *E*_{corr} of the bare OL electrode is -501.5 mV and the corresponding corrosion current density *i*_{corr} is 0.9329 mA / cm². In the case of the deposition with the highest *IE*, *E*_{corr} presents the largest value from all the analyzed electrodes obtained values, -401 mV, and *i*_{corr} is 0.2745 mA / cm².

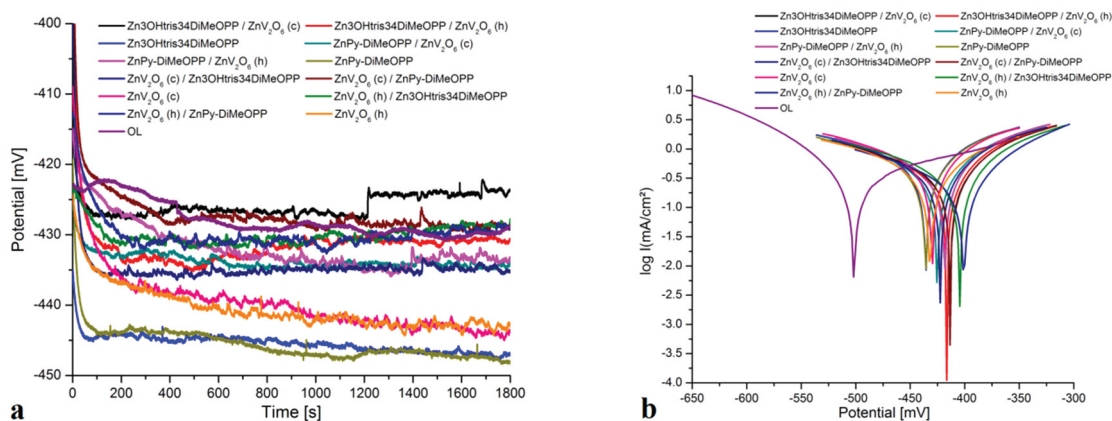


Figure 3 a) Evolution of OCP with time for investigated electrodes in 0.1 HCl solution for the realized depositions; b) Tafel representation of polarization curves recorded in 0.1 M HCl for the studied electrodes

It can be also noticed that the corrosion current intensity values of carbon steel material in 0.1 M HCl solution decrease from 0.93 mA / cm² for bare OL for all the depositions going to the lowest value of 0.27 mA / cm² for the ZnV₂O₆ (h) / ZnPyDiMeOPP which offers the best inhibition efficiency in relationship with the capacity of this porphyrin to develop non-planar conformations and to form high aggregates with kwatarionic architectures.

Table 3 The Tafel parameters of investigated electrodes after 30 minutes immersion in 0.1 M HCl solution

Electrode	E_{corr} (mV)	R_p ($\Omega \cdot \text{cm}^2$)	i_{corr} (mA / cm ²)	V_{corr} (mm / y)	IE (%)
OL	-501.5	64.54	0.9329	3.210	-
ZnV ₂ O ₆ (h)	-431.9	53.76	0.5047	5.903	45.89
ZnV ₂ O ₆ (c)	-429.9	38.98	0.4904	5.735	47.43
ZnPy-DiMeOPP	-435.9	43.80	0.4790	5.602	48.65
Zn3OHtris34DiMeOPP	-435.8	40.56	0.5331	6.235	42.85
ZnV ₂ O ₆ (h) / ZnPyDiMeOPP	-401.0	76.85	0.2745	3.210	70.58
ZnV ₂ O ₆ (h) / Zn3OHtris34DiMeOPP	-404.8	60.81	0.3788	4.430	58.97
ZnV ₂ O ₆ (c) / ZnPyDiMeOPP	-413.4	58.88	0.3271	3.825	64.93
ZnV ₂ O ₆ (c) / Zn3OHtris34DiMeOPP	-422.3	53.80	0.3747	4.382	59.83
ZnPy-DiMeOPP / ZnV ₂ O ₆ (h)	-418.4	49.95	0.4460	5.216	52.19
ZnPy-DiMeOPP / ZnV ₂ O ₆ (c)	-425.3	53.10	0.4256	4.978	54.37
Zn3OHtris34DiMeOPP / ZnV ₂ O ₆ (h)	-416.5	57.11	0.3650	4.269	60.87
Zn3OHtris34DiMeOPP / ZnV ₂ O ₆ (c)	-413.3	57.48	0.3412	3.991	63.42

4. CONCLUSION

ZnV₂O₆ nanomaterial was successfully obtained using two different synthesis methods. ZnV₂O₆, ZnPyDiMeOPP and Zn3OHtris34DiMeOPP porphyrins were deposited in single or sandwich structures on carbon steel electrodes. The surface and the morphologies of the deposition were analyzed using microscopic SEM and AFM techniques. The electrochemical measurements for the deposited layers revealed that the best results regarding the inhibition efficiency (70.58%) of the deposited layers on carbon steel disks were obtained in the case of the sandwich structure with the first layer consisting in ZnV₂O₆ hydrothermally obtained and ZnPy-DiMeOPP porphyrin as the second layer. Also, it was determined that the sandwich structures depositions

present a better *IE* than single layers depositions. The fact that porphyrin above the oxide is the best covering layer for corrosion inhibition might be explained by the capacity of porphyrins to be distorted from planar structure, creating in this way thicker layers that are more protective because of kwatarionic architectures.

ACKNOWLEDGEMENTS

The authors kindly acknowledge the PN III No. 107 PED / 2017 project - CorOxiPor: Nanostructured anticorrosive hybrid materials based on pseudo-binary oxides and Zn-metalloporphyrins.

REFERENCES

- [1] ALI, A., FALIH, S., YOUSIF, N., REZGAR, R., KAMAL, I., Modeling and Optimization of Structural Steel Corrosion Inhibition using barely Grass Extract as Green Inhibitor, *American Journal of Environmental Engineering*, 2017, vol. 7, no. 4, pp. 73-81.
- [2] BOUSSKRI, A., ANEJJAR, A., JODEH, S., BELKHAOUA, M., Investigation of the Inhibition Effect of 1-(2-(4-Nitro Phenyl) 2-oxoethyl)-4-N-Methyl) Picolinium Bromide on Carbon Steel Corrosion in Hydrochloric Acid Medium, *Applied Journal of Environmental Engineering Science*, 2017, vol. 3, pp. 96-113.
- [3] AIT HADDOU, B., CHEBABE, D., EL ASSYRY, A., DERMAJ, A., TOUIL, M., IBN AHMED, S., HAJJAJI, N., Experimental and theoretical investigation of 3-methyl-1,2,4-triazole-5-thione derivatives as inhibitors for mild steel corrosion in acid medium, *Journal of Materials and Environmental Sciences*, 2017, vol. 8, no. 11, pp. 3943-3952.
- [4] GONZALEZ-RIVERA, Y. A., MEZA-ROCHA, A. N., AQUINO-MENESES, L., JIMENEZ-SANDOVAL, S., RUBIO-ROSAS, E., CALDINO, U., ALVAREZ, E., ZELAYA-ANGEL, O., TOLEDO-SOLANO, M., LOZADA-MORALES, R., Photoluminescent and electrical properties of novel Nd³⁺ doped ZnV₂O₆ and Zn₂V₂O₇, *Ceramics International*, 2016, vol. 42, no. 7, pp. 8425-8430.
- [5] LIU, H., TANG, D., Synthesis of ZnV₂O₆ powder and its cathodic performance for lithium secondary battery, *Materials Chemistry and Physics*, 2009, vol. 114, pp. 656-659.
- [6] SUN, Y., LI, C.-S., YANH, Q.-R., CHOU, S.-L., LIU, H.-K, Electrochemically active, novel layered m-ZnV₂O₆ nanobelts for highly rechargeable Na-ion energy storage, *Electrochimica Acta*, 2016, no. 205, pp. 62-69.
- [7] TANG, R., LI, Y., LI, N., HAN, D., LI, H., ZHAO, Y., GAO, C., ZHU, P., WANG, X., Reversible Structural Phase Transition in ZnV₂O₆ at High Pressures, *The Journal of Physical Chemistry C*, 2014, vol. 118, no. 20, pp. 10560-10566.
- [8] AHAMAD, I., PRASAD, R., QURAIISHI, M. A., Thermodynamic, electrochemical and quantum chemical investigation of some Schiff bases as corrosion inhibitors for mild steel in hydrochloric acid solutions, *Corrosion Science*, 2010, vol. 52, pp. 933-942.
- [9] LOKESH, K. S., DE KEERSMAECKER, M., ADRIAENS, A., Self-assembled films of porphyrins with amine groups at different positions: Influence of their orientation on the corrosion inhibition and the electrocatalytic activity, *Molecules*, 2012, vol. 17, pp. 7824-7842.
- [10] BIRDEANU, M., BÎRDEANU, A. - V., POPA, I., TARANU, B., PETER, F., CREANGA, I., PALADE, A., FAGADAR-COSMA, E., Comparative research regarding corrosion protective effect of different sandwich type nanostructures obtained from porphyrins and pseudo-binary oxides by changing the deposition order, in NANOCON 2014: 6th International Conference on Nanomaterials, Brno, Czech Republic, 2014, pp. 262-268.
- [11] FAGADAR-COSMA, E., LASCU, A., PALADE, A., CREANGA, I., FAGADAR-COSMA, G., BIRDEANU, M., Hybrid material based on 5-(4-pyridyl)-10,15,20-tris(4-phenoxyphenyl)-porphyrin and gold colloid for CO₂ detection, *Digest Journal of Nanomaterials and Biostructures*, 2016, vol. 11, no. 2, pp. 419-424.
- [12] AHMAD, Z. Principles of Corrosion Engineering and Corrosion Control, Butterworth-Heinemann / IChemE Series. Elsevier, Amsterdam. 2006. page 377.